Review

John F. Honek*

Glyoxalase biochemistry

DOI 10.1515/bmc-2015-0025
Received August 22, 2015; accepted October 1, 2015

Abstract: The glyoxalase enzyme system utilizes intracellular thiols such as glutathione to convert α-ketoaldehydes, such as methylglyoxal, into D-hydroxyacids. This overview discusses several main aspects of the glyoxalase system and its likely function in the cell. The control of methylglyoxal levels in the cell is an important biochemical imperative and high levels have been associated with major medical symptoms that relate to this metabolite's capability to covalently modify proteins, lipids and nucleic acid.

Keywords: advanced glycation end-products; detoxification; DNA modification; glutathione; glyoxalase; methylglyoxal; protein post-translational modification.

Introduction

The glyoxalase enzyme system is a group of enzymes that overall convert α-ketoaldehydes into D-hydroxyacids (1–5). In the case of methylglyoxal (MG), D-lactate is the product. There are several glyoxalase enzymes that have been identified. Glyoxalase I (Glo1) converts a non-enzymatically formed hemithioacetal, the adduct between an intracellular thiol such as glutathione (GSH) and a metabolically produced α-ketoaldehyde such as MG, into a thioester product (Figure 1) (6–9). In the case of MG and GSH, *S*-D-lactoylglutathione is the product. Glyoxalase II (Glo2) hydrolyzes this thioester into D-lactate and regenerates the intracellular thiol GSH. Glo1 and Glo2 work in tandem to convert cytoxic MG into D-lactate. Interestingly, it has been determined that another enzyme, termed glyoxalase III (Glo3) is capable of directly converting MG into D-lactate/L-lactate, depending on the source of the enzyme (10–12) (Figure 1). The continuing focus on these enzymes, their structure-function, and their identification from various biological sources is an important area of biochemistry. Studies on the biochemistry of MG, its reaction with biomolecules in the cell, the analysis of these modifications, and the resulting cellular and physiological outcomes are also of major concern (13–16). This area of biochemistry has continued to be of interest as evidenced by a recent international conference organized by the Biochemical Society in 2013 celebrating the 100-year anniversary of glyoxalase research. The resulting publications from that conference are highly recommended to the reader (17–19). The overview presented in this current article hopes to capture the major themes of research in this area and also provide additional recent literature (to August 2015) to add to the reader's appreciation of this field.

***Corresponding author: John F. Honek,** Department of Chemistry, University of Waterloo, 200 University Avenue West, Waterloo N2L 3G1, Ontario, Canada, e-mail: jhonek@uwaterloo.ca

Methylglyoxal

MG is present in all cells and its concentration at any moment is a result of its production by both non-enzymatic (major) and enzymatic mechanisms as well as its degradation by the glyoxalase enzymes and other enzymes of varying importance capable of oxidatively or reductively metabolizing it (20–23). Non-enzymatic conversion of triose phosphates such as dihydroxyacetone phosphate (DHAP) and glyceraldehyde-3-phosphate (GAP), which are normal intermediates in the glycolytic pathway, can occur in aqueous solutions which can complicate the determination of MG concentrations and glycation labeling in biological solutions and tissues (24–26) (Figure 2). Indeed, the non-enzymatic conversion of triose phosphates to MG in cells is considered to be the major contributor to MG cellular levels. Mechanistically, the removal of a proton alpha to the carbonyl present in DHAP/GAP results in the elimination of inorganic phosphate through the intermediacy of the enediolate phosphate, 3-phospho-2, 3-ene-diol. The glycolysis pathway enzyme triose phosphate isomerase (TIM) increases the observed rate of MG formation in the presence of DHAP/GAP as this enzyme catalyzes the net conversion of DHAP to GAP, GAP having a higher rate of non-enzymatic elimination of inorganic phosphate than DHAP to form MG (25, 26). In rat tissues, MG formation has been estimated to be approximately 0.4 mM per day taking

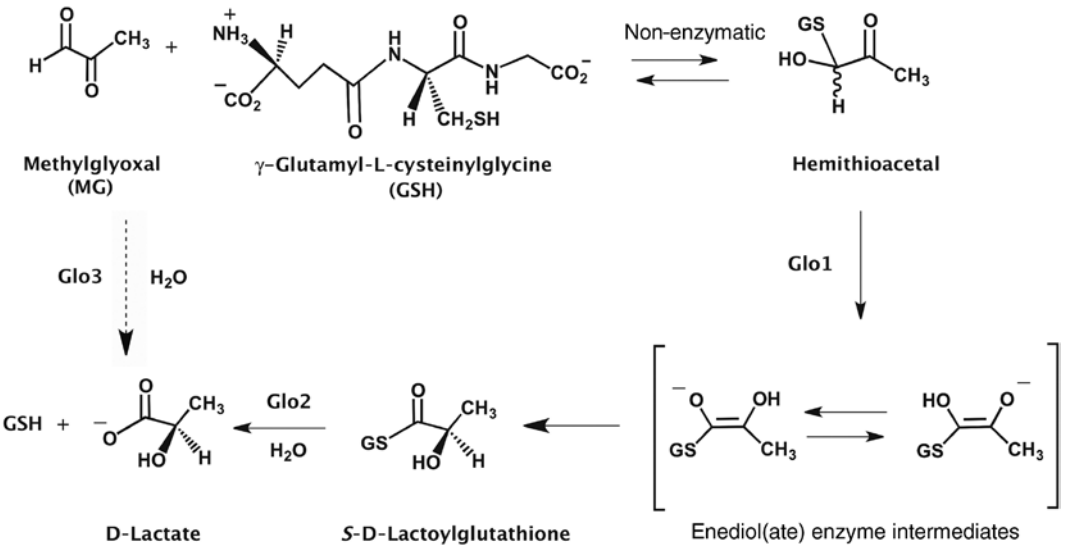

Figure 1: Reaction schemes for the glyoxalase enzymes.

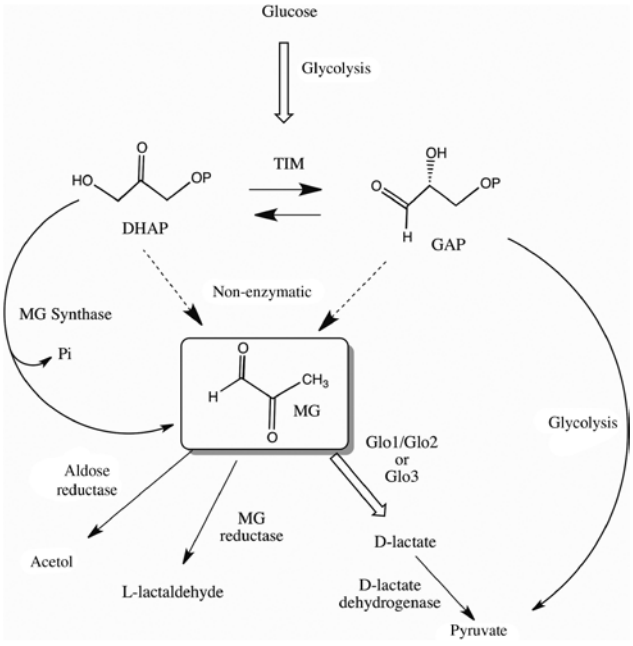

Figure 2: Some of the biological pathways that lead to and from MG including the position of the enzymes Glo1, Glo2 and Glo3.

into account contributions by TIM (26). In humans the whole body rate of formation of MG has been estimated to be approximately 3 mmol per day (16). The glyoxalase system and various aldo-keto oxidoreductases metabolize the MG, and substantially, but not completely, protect cells from MG toxicity (14, 27, 28).

Enzymatic formation of MG is also known, and these organism-dependent pathways vary in their overall contribution to MG production. A direct enzymatic route for the production of MG through the activity of the enzyme MG synthase has been identified in *Escherichia coli* (29–31). The enzyme catalyzes MG formation from DHAP (Figure 2). Triose phosphate isomerase-deficient mutants of *E. coli* were observed to accumulate MG in these bacteria. MG synthase has been isolated and it has been hypothesized that in concert with the glyoxalase system, the resulting D-lactate is converted to pyruvate by the bacterial enzyme D-lactate dehydrogenase. The overarching metabolic scheme (MG → → pyruvate) bypasses the formation of pyruvate by the usual glycolytic pathway (Figure 2). Inorganic phosphate (P_i) was observed to inhibit the *E. coli* MG synthase, an observation that suggested that this "glycolytic bypass" is likely activated in *E. coli* under environmental conditions where (P_i) is limiting (29). The redirection of DHAP consumption occurring in the "glycolytic bypass" would conserve the existing Pi cellular pool, thus permitting Pi-dependent phosphorylation steps such as that found in the GAP dehydrogenase catalyzed reaction in glycolysis to continue. Threonine catabolism can yield MG through the intermediacy of aminoacetone, which is subsequently oxidized to MG by a monoamine oxidase (32). MG has also been shown to be a product from the oxidation of acetone (acetone → acetol → MG) as catalyzed by select cytochrome P450 enzymes (33, 34).

Aldo-keto oxidoreductases

As will be discussed below, MG is a highly electrophilic molecule and can covalently label proteins/enzymes,

DNA, and other biomolecules. In order to avoid the cytotoxicity of MG and that of other α-ketoaldehydes such as glyoxal, phenylglyoxal and hydroxypyruvaldehyde, cells have developed enzymatic systems to metabolize MG. One set of enzymes is the aldo-keto oxidoreductases. NADPH-dependent oxidoreductases that catalyze the conversion of MG to acetol or lactaldehyde have been identified in various bacteria and mammals (35–38). MG reductase has been identified in fungi and in mammalian liver homogenates and catalyzes the conversion of MG to lactaldehyde (39–41). Some *Clostridia* species utilize the enzyme glycerol dehydrogenase to decrease cellular MG concentrations by first reducing MG to acetol likely by an aldose reductase, which is followed by reduction to 1,2-propanediol by glycerol dehydrogenase (42). It has been suggested that the protozoan *Trypanosoma brucei* utilizes an MG reductase to detoxify this compound, resulting in the production of *L*-lactaldehyde, although some uncertainty in this proposal has been expressed. It is clear however, that the enzyme Glo1 is not present in this organism (22, 43, 44).

Glyoxalase enzymes

Another set of enzymes that play a role in protecting cells from the cytotoxicity of MG is the glyoxalase set of enzymes. These enzymes make a major contribution to MG detoxification in most cells.

Glo1

The most extensively investigated glyoxalase enzymes are Glo1 and Glo2. Glyoxalase I (Glo1; *S*-D-lactoylglutathione MG lyase (isomerizing); EC 4.4.1.5) is the first of a pair of enzymes of the glyoxalase enzyme system that work in tandem to convert MG to D-lactate (Figure 1). The substrate for Glo1 is the hemithioacetal, formed non-enzymatically from the nucleophilic reaction between the cellular tripeptide GSH and MG (23, 44–46). It should be pointed out that a recent study on yeast Glo1 has indicated that the best fit to the experimental kinetic data was the situation where a GSH-Glo1 binary complex was formed initially in the active site of the yeast enzyme with subsequent binding of MG to form the ternary complex hemithioacetal in the active site of the enzyme (47). These interesting initial findings warrant further investigation and a determination as to whether this mechanism also extends to Glo1 enzymes from other organisms.

Numerous Glo1 enzymes are widespread in nature, yet a few organisms appear not to harbor a Glo1 enzyme. Although *T. brucei* appears to lack Glo1 (although *T. brucei* is suggested to have a MG reductase that reduces MG to *L*-lactataldehyde as mentioned previously), *T. cruzi* does contain an active Glo1 (44, 48, 49). *Giardia lamblia* and *Entamoeba histolytica* however, lack Glo1 based on genome analyses (49). The predominant use of the glyoxalase enzymes to detoxify MG and other reactive dicarbonyls has resulted in intense interest in ameliorating our understanding of the structure-function relationships of these enzymes. Early research had shown that Glo1 is a Zn^{2+}-activated metalloenzyme when isolated from biological sources such as yeast, mammals, and *Pseudomonas putida* (7, 50–52). Nevertheless, metal ions such as Co^{2+}, Mn^{2+}, Ni^{2+}, and even Mg^{2+} were also found to activate the Glo1 isolated from these sources (53). This foundational research indicated a broad metal promiscuity for Glo1, although metal reconstitution experiments were technically challenging at times.

The X-ray structure of the homodimeric Glo1 from *Homo sapiens* bound to the inhibitor S-benzylglutathione provided the first detailed structural information on a Glo1 (54) (Figure 3). Two active sites each bound to octahedral Zn^{2+} were detected. Each Zn^{2+} was liganded by two amino

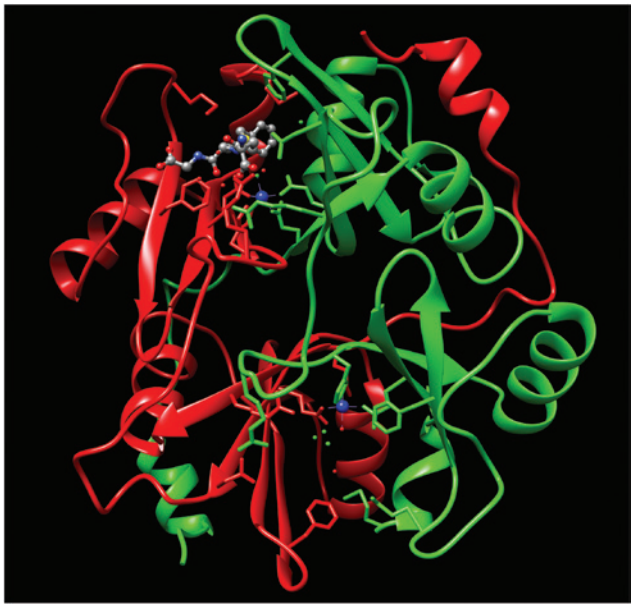

Figure 3: Ribbon representation of *H. sapiens* glyoxalase I with S-benzylglutathione inhibitor bound to the active site.
The two subunits of the enzyme are colored green and red. Active site hexacoordinate Zn^{2+} is shown as a blue sphere with amino acid side chains from both subunits contributing to the binding of each active site zinc atom. The inhibitor (in ball-and-stick) is only shown in one active site for clarity. (PDB code: 1FRO).

acid residues from one subunit (His127, Glu173) and two residues (Gln34, Glu100) from the second subunit. Water molecules were also found proximal to the Zn^{2+} center and were likely liganded to the metal ion in the absence of the inhibitor. This information provided structural confirmation of previous biophysical studies that indicated that Glo1 maintains an octahedral metal coordination environment, with metal-bound H_2O/OH^- also participating (55–57). Although also expecting the isolated *Escherichia coli* Glo1 to be a Zn^{2+}-activated enzyme, a surprising metal activation profile was observed for this enzyme, drastically different from previously studied Glo1 (58). A narrower metal activation profile was observed for the *E. coli* Glo1, with Ni^{2+} reconstitution providing the most active enzyme. Co^{2+} resulted in a lower activity Glo1 and Cd^{2+} and Mn^{2+} ions activated the enzyme to only modest levels. Surprisingly, no enzyme activity was observed in the presence of Zn^{2+}, a very different and unexpected characteristic.

Extended X-ray Absorption Fine Structure (EXAFS), X-ray Absorption Near Edge Structure (XANES) and X-ray crystallographic structure data were obtained on the *E. coli* Glo1 enzyme (59–61) (Figure 4). The enzyme is homodimeric in quaternary structure, which is similar to the *H. sapiens* Glo1. Analyses of the *E. coli* Glo1 structural data showed two active sites, each active site being formed by contributions from residues from each of the two subunits (Chain A: His74, Glu122; Chain B: His5, Glu56) with two water (or hydroxide) molecules present that complete the octahedral metal coordination. All metal ions that activated *E. coli* Glo1 had octahedral geometry in the active site of the enzyme. Zn^{2+}, which did not activate the *E. coli* enzyme, did indeed bind. However, the coordination geometry was found to be close to trigonal bipyramidal, with only one H_2O/OH^- bound to the zinc center. Subsequent studies by nuclear magnetic resonance spectroscopy (NMR) elaborated on the inequivalence of the two active sites in the *E. coli* enzyme, accounting for previous solution studies (58, 62, 63). Additional studies on substrate thiol structure-function activities and kinetic isotope effects were reported for the *E. coli* Glo1 (64).

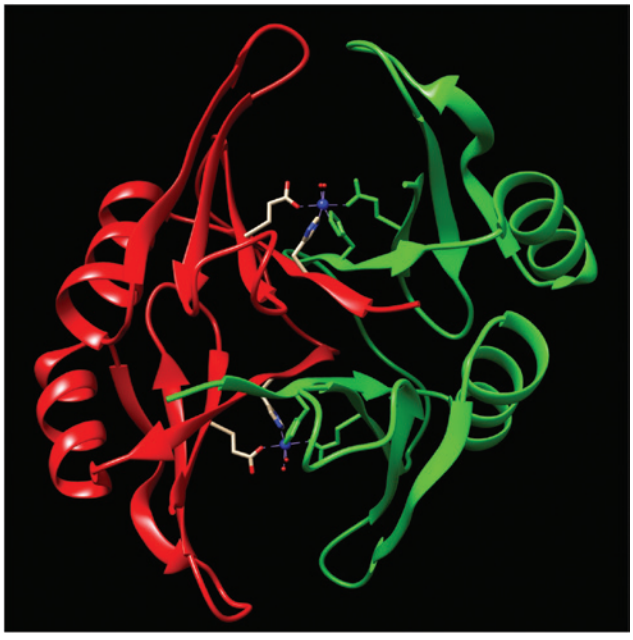

Figure 4: Ribbon representation of *E. coli* glyoxalase I.
The two subunits of the enzyme are colored green and red. Active site hexacoordinate Ni^{2+} is shown as a blue sphere with amino acid side chains from both subunits contributing to the binding of each active site nickel atom. Two water molecules shown as red spheres complete the active site metal coordination. (PDB 1F9Z).

Investigations of the metal-activation profiles for other Glo1 enzymes provided additional support for the two classes of Glo1. For example, the *Leishmania major* Glo1 was reported to lack Zn^{2+}-activation, but was found to be fully active in the presence of Ni^{2+} ion (48). Additionally this enzyme was found to utilize the cellular thiol trypanothione (bis(glutathionyl)spermidine) as the thiol co-substrate for the enzyme (Figure 5). This thiol is exclusively found in parasitic protozoa of the order Kinetoplastida, such as trypanosomes and leishmania (44). Several of these organisms are the causative agents of certain human diseases such as Chagas disease and leishmaniasis. Other Ni^{2+}-activation class Glo1 have been found in *T. cruzi* and *Leishmania donovani* (22, 65, 66). Recently a Glo1 utilizing the intracellular thiol bacillithiol was identified in *Bacillus subtilis* (67) (Figure 5). Studies investigating the metal activation characteristics of other bacterial Glo1 have also provided evidence for the existence of the Ni^{2+}-activation class. For example, Glo1 from *Neisseria meningitides*, *Yersinia pestis*, and *Pseudomonas aeruginosa* PAO1 were all found to substantially exhibit the same metal activation profiles as seen with the Glo1 from *E. coli* (68). Subsequently, two other open reading frames (ORFs) coding for putative Glo1 enzymes in the *P. aeruginosa* PAO1 genome were identified, and their gene products overproduced and studied (69). The Glo1 activity of the two additional putative Glo1 were confirmed in these studies. One of these Glo1 is shorter in length and has higher amino acid sequence homology to the *E. coli* and the first identified *P. aeruginosa* Glo1. This Glo1 exhibits the characteristics of the Ni^{2+}-activation class enzymes, with no evidence for Zn^{2+} activation (the X-ray structure of this enzyme has recently been reported) (70). The third Glo1 has a longer amino acid sequence and a higher amino acid sequence homology to the human and the *Pseudomonas putida* Glo1, which are known Zn^{2+}-activation class enzymes. This

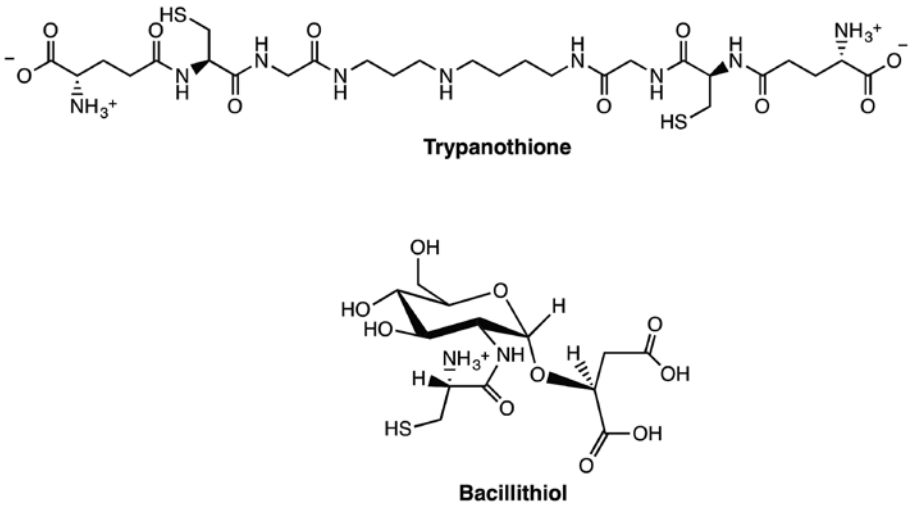

Figure 5: Chemical structures of trypanothione and bacillithiol.

enzyme was found to be activated by Zn^{2+} and exhibited the "classic" promiscuous metal activation profile typical of the Zn^{2+}-activation class of Glo1 enzymes. Little is currently known about the physiological importance of the presence of three Glo1 in *P. aeruginosa* PAO1, nor the possibility of differential expression of the Glo1s under various growth conditions. Although much speculation has centered on what mechanisms are used by Glo1 to control its metal specificity, a recent investigation has clearly delineated the contributions of various structural components to the metal-activation profile exhibited by Glo1 (71). Using deletional mutagenesis on the Zn^{2+}-activated Glo1 enzyme from *P. aeruginosa*, researchers were able to completely switch the metal-activation class of the enzyme, to one where selective Ni^{2+} activation was exhibited. This research contributes to our further understanding of metalloenzymes and of Glo1 metal specificity in particular.

Based on the quaternary structures and the subunit arrangements found for Glo1 enzymes for which X-ray structures had already been determined, it was assumed that, for homodimeric Glo1 enzymes, each of the two active sites would depend on amino acid residues from each of the two subunits to supply the metal ligating residues. This is clearly seen in the *H. sapiens* and the *E. coli* Glo1 X-ray structures (54, 61). Surprisingly, an alternate subunit orientation from the homodimeric subunit arrangement found in the *H. sapiens* and *E. coli* Glo1 was discovered as a result of structural genomics initiatives. The X-ray structure of the Glo1 enzyme from *Clostridium acetobutylicum*, which was found to exhibit Ni^{2+}-activation class properties, was determined. Although the *C. acetobutylicum* Glo1 was confirmed to be dimeric by gel permeation chromatography, the X-ray structures determined for both the Zn^{2+}-bound (inactive) and the Ni^{2+}-activated Glo1 exhibited very different orientations of the subunits compared to the arrangements found in the *H. sapiens* and the *E. coli* Glo1 enzymes (72) (Figure 6). Both of these metallated forms of the *C. acetobutylicum* Glo1 have two active sites yet each active site is formed by contribution from *only one* of the subunits. All the amino acid residues that ligate a particular Ni^{2+} atom are contributed by only a single protein subunit. Yet the arrangements of coordinating ligands around the Ni^{2+} center are almost superimposable with those from the *E. coli* Glo1 enzyme. From these results, it is clear that Glo1 can maintain the required catalytically active octahedral geometry around the active site metal ion, yet provide that environment in two completely different ways. These results exemplify the capability of Nature to supply alternative scaffolds to construct identical active sites. It should also be noted that not all Glo1 enzymes are homodimeric. For example, the Glo1 from *Saccharomyces cerevisiae* and *Plasmodium falciparum* are both monomers, but have molecular weights that are double that of a "standard" subunit of a multisubunit Glo1 enzyme such as *E. coli* (73, 74). The *S. cerevisiae* Glo1 has two functioning active sites, each exhibiting slightly different kinetic properties and possibly metal activation profiles. On the other hand, it has been reported that the *P. falciparum* Glo1 exhibits allosterically coupled active sites having different substrate affinities (75). Recent reports have identified additional Ni^{2+}-activation class Glo1 enzymes in plant systems, including single subunit enzymes of the same size as the *S. cerevisiae* and the *P. falciparum* Glo1 (76–79). These findings are being actively studied with respect to stress response systems in agricultural important crops, and should prove extremely important in addressing the

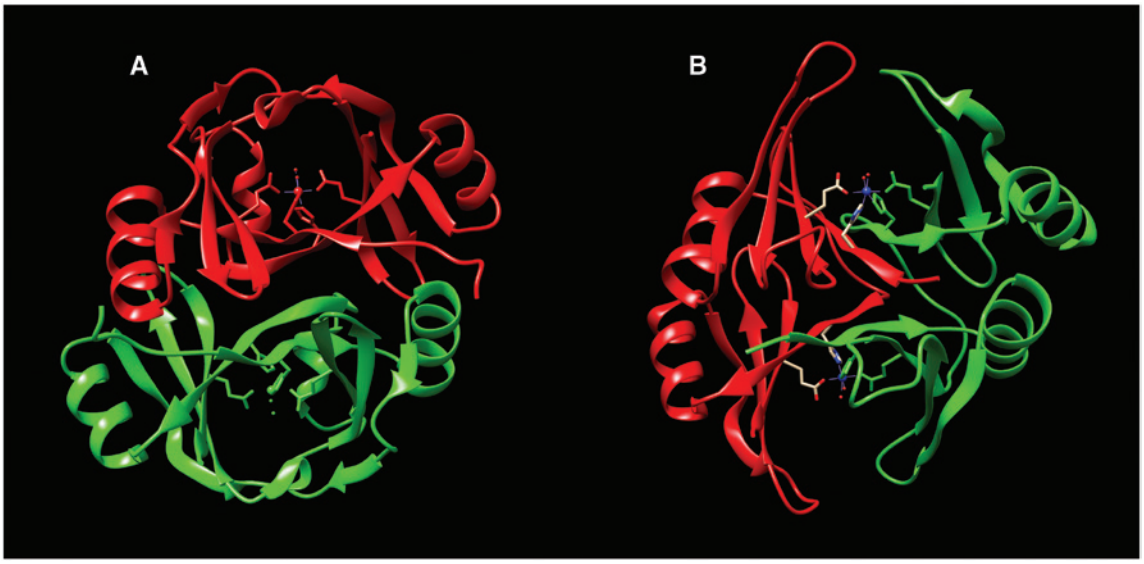

Figure 6: X-ray structure of Glo1 from *Clostridium acetobutylicum* (A) and Glo1 from *Escherichia coli* (B).
Note the close similarities in their active sites but the orientation differences of the two subunits between the two enzymes. (PDB: 3HDP and 1F9Z).

effects of climate change and increasing global population on future food availability (78).

An additional aspect to the overall molecular structure of the Glo1 enzymes is that their protein fold is shared by other proteins in its structural class (βαββββ structural superfamily) yet these proteins exhibit a range of biological activities (54, 80, 81). Each protein subunit from a homodimeric Glo1 enzyme such as that from *H. sapiens* or *E. coli* is composed of two βαββββ structural domains. For the extended single chain Glo1 from *S. cerevisiae* and *P. falciparum*, based on protein homology modeling, four βαββββ domains are likely present. It has been proposed that the evolution of new structures and functions within this protein family likely arose from a combination of horizontal gene transfer and gene fusion events and possibly gene duplication events (79, 81). The possibility of three-dimensional domain swapping has also been proposed (52, 54). It is interesting to note that the Glo1 protein fold is also found in several βαββββ structural superfamily members that are involved in antibiotic resistance (82). Several of these proteins are important to the resistance of the antibiotic producing organism to the cytotoxic natural product that it produces. The resistance proteins usually act by binding the cytotoxic compound preventing cellular toxicity to the antibiotic producing organism, until the toxin can be controllably released outside the cell. For example, the bleomycin resistance protein from *Streptoalloteichus hindustanus* (83), the *Streptomyces lavendulae* mitomycin C resistance protein (84) and the thiocoraline peptide binding protein produced by strains of *Micromonospora* (85), all act to bind a cytotoxic molecule, lowering its toxicity to the antibiotic producing organism. These proteins have high structural similarity to Glo1. On the other hand, the fosfomycin resistance proteins (Fos A, B and X) are also structurally related to Glo1 but act by chemically degrading the reactive epoxide functionality in the antibiotic fosfomycin (82, 86, 87) (Figure 7). Fos A, B and X are metalloenzymes and use either intracellular thiols or water to accomplish the epoxide ring opening.

Glo2

S-D-Lactoylglutathione is the product of the Glo1-catalyzed reaction if MG is the dicarbonyl substrate (Figure 1). The resulting thioester is the substrate for the hydrolytic reaction catalyzed by glyoxalase II (Glo2;

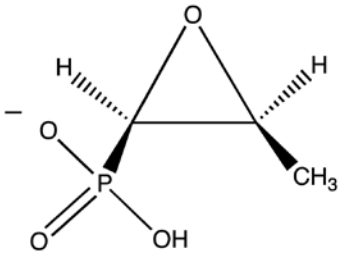

Figure 7: Chemical structure of the antibiotic fosfomycin.

S-2-hydroxyacylglutathione hydrolase, EC 3.1.2.6). In general, Glo2 hydrolyzes various α-hydroxythioesters to their non-cytotoxic α-hydroxycarboxylic acids, regenerating GSH. In the case of MG, D-lactate is produced after enzymatic conversion by the Glo1 and Glo2 enzyme pair. Three dimensional protein structures for a variety of Glo2 representatives have been reported and include Glo2 from *H. sapiens, Arabidopsis thaliana, Leischmania infantum and Salmonella typhimurium* (Figure 8) (88–91). In several organisms, two or more Glo2 enzymes have been identified and appear to differentially localize in cellular compartments such as the mitochondria and apicoplast depending on the particular organism (44, 92, 93). Glo2 is a binuclear metalloenzyme with Zn^{2+} as the frequently detected active site metal ion. The cytosolic and the mitochondrial Glo2 from *A. thaliana*, however, have been reported to contain varying ratios of Zn^{2+}, Fe^{2+} and Mn^{2+} and exhibit broad metal activation, although it has been reported that the Zn^{2+}/Fe^{2+} binuclear center is essential for optimal catalysis (94, 95). Ni^{2+} and Co^{2+} are also activating metal ions for the enzyme, depending upon the specific Glo2. The human Glo2 has also been shown to contain a mixed binuclear center with Zn^{2+} and Fe^{2+} present, although the mononuclear Zn^{2+} reconstituted enzyme is also active (96). As *E. coli* Glo1 was previously shown to be in a separate Glo1 metal activation class, that of the Ni^{2+}-activation class, a study of *E. coli* Glo2 was undertaken to determine if the metal specificity of this enzyme was also unusual (97). The *E. coli* Glo2 enzyme was isolated with approximately two moles of Zn^{2+} bound per mole of active enzyme. Metal reconstitution studies were undertaken on the apoenzyme form of the *E. coli* Glo2. Activity regain was observed for reconstitution of the enzyme with either Mn^{2+} or Co^{2+} but not Ni^{2+}, indicating that Ni^{2+} activation was not observed in Glo2 as it was for the *E. coli* Glo1 enzyme. Hence Ni^{2+} activation is not a profile that occurs for both the Glo1 and the Glo2 enzyme pair in *E. coli*. A second Glo2, Glo2-2 (also termed GlxII-2) has just been reported from *E. coli* and makes a contribution to MG resistance in this organism, although it has a lower activity against the substrate, *S*-D-lactoylglutathione (98).

The Glo2 molecular structures share the same overall fold as the Zn^{2+}-dependent metallo-β-lactamases, which are members of the larger Zn^{2+}-metallohydrolase structural family of proteins (99, 100). The Glo2 enzyme is monomeric. Recent work has probed the substrate specificity variation with alteration of the metal reconstitution of various metallohydrolase protein family members, including Glo2 (101). The authors concluded that promiscuous activities of metalloenzymes can stem from an ensemble of metal isoforms in the cell, which could facilitate the functional divergence of metalloenzymes and engender new activities for the cell. The structural relatedness of family members in this superfamily has been nicely underscored by the conversion of a Glo2 into a functioning β-lactamase through protein evolution (102).

Figure 8: X-ray structure of the *H. sapiens* Glo2 with the binuclear Zn^{2+} atoms shown as blue spheres (PDB: 1QH5).

Glo3

Although Glo1 and Glo2 are major contributors to the metabolism of MG and likely other electrophilic dicarbonyl compounds formed within the cell, another protein exhibiting glyoxalase activity in *E. coli* has been identified (11). The enzyme, Glo3 (EC 4.2.1.130), was observed to directly convert MG into a D-lactate/L-lactate mixture without the necessity of a small molecular weight thiol such as GSH (12). Studies have shown that this enzyme functions as a heat-shock inducible chaperone, termed Hsp31 in *E. coli*, and is regulated by the RNA polymerase sigma factor (RpoS) (103, 104). A corresponding homolog is present in *H. sapiens* and is termed DJ-1, also exhibiting glyoxalase activity (105). Related proteins with Glo3 activities have been identified in yeasts, mice and the worm *Caenorhabditis elegans* (10, 105). It appears therefore that these chaperone proteins, which are usually noted for their ability to reduce protein folding errors and protein aggregation in the cell, may have a secondary role in handling reactive dicarbonyl compounds. The Glo3/Hsp31 *E. coli* protein is

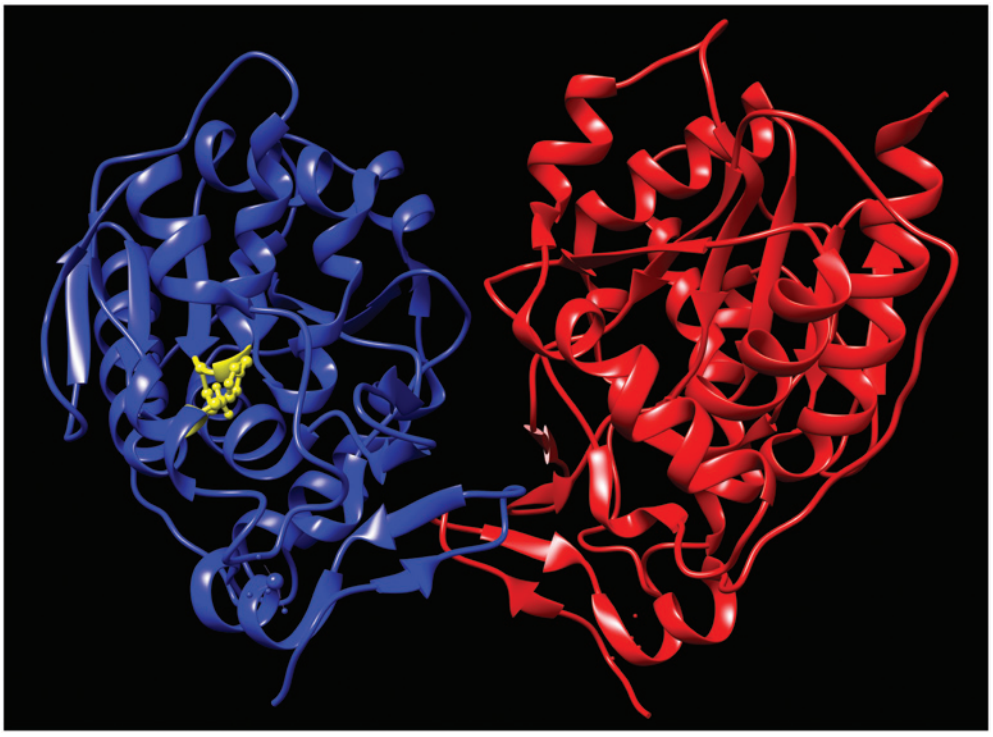

Figure 9: X-ray structure of homodimeric *E. coli* Hsp31/Glo3 with two subunits colored in red and blue.
The active site containing Cys184, His185 and Asp213 as shown in one of the subunits in ball-and stick (yellow) (PDB:1N57).

homodimeric in nature and has a native molecular mass of approximately 82 kDa (Figure 9) (11, 106). The *E. coli* Hsp31, *H. sapiens* DJ-1 and yeast YDR533Cp proteins have related structures and similar potential active sites, with Cys, His Glu/Asp residues present and a possible metal binding site. This molecular arrangement would likely favor reaction of the cysteine thiol with the electrophilic carbonyl of MG, aiding in the subsequent isomerization of the covalent MG-protein adduct to a thioester, with subsequent hydrolysis of this thioester intermediate (12).

It is clear that structural investigations on the glyoxalase enzymes can lead to new fundamental knowledge not only in the area of cellular physiology and MG toxicity but also in other areas such as antibiotic resistance and Hsp/chaperone biochemistry.

Advanced glycation end-products (AGE) and the dicarbonyl proteome

The buildup of MG is a deleterious situation for a cell, with drastic consequences to its normal homeostasis and even its viability (16, 20, 21, 107). The electrophilic nature of dicarbonyls, such as MG, dictates the nature of their interactions with biomolecules such as proteins, DNA, RNA and cellular membranes. Due to the extreme reactivity of the dicarbonyl functionality, multiple cellular sites can be modified, termed advanced glycation end-products (AGE), and the ensuing cellular state will be a composite of the additive/synergistic effects that result from the array of modified cellular targets (14, 108). The glyoxalase enzymes, along with other detoxification enzymes such as the aldoketo reductases, play critical roles in the removal of dicarbonyl compounds before they can react with molecular targets and produce cellular toxicity. Studies have attempted to identify the nature of the chemical modifications that are produced in the presence of MG and to quantitate their presence (16, 18, 109–112). Further research has contributed to the identification of some of the molecular targets labeled by MG and to the careful evaluation of the impact that these modifications have on human health.

The nature of several protein and nucleic acid modification reactions has been elucidated and, in the case of MG, reactions with arginine and lysine side chains are found to predominate for proteins (20, 33, 109, 110, 113, 114) (Figure 10). A range of chemical reactions has been found to occur with arginine side chains, the MG-H1 adduct is thought to be the most frequent arginine glycation modification, although several other adducts have been identified and include MG-H2, MG-H3, tetrahydropyrimidine (THP) and the fluorescent adduct

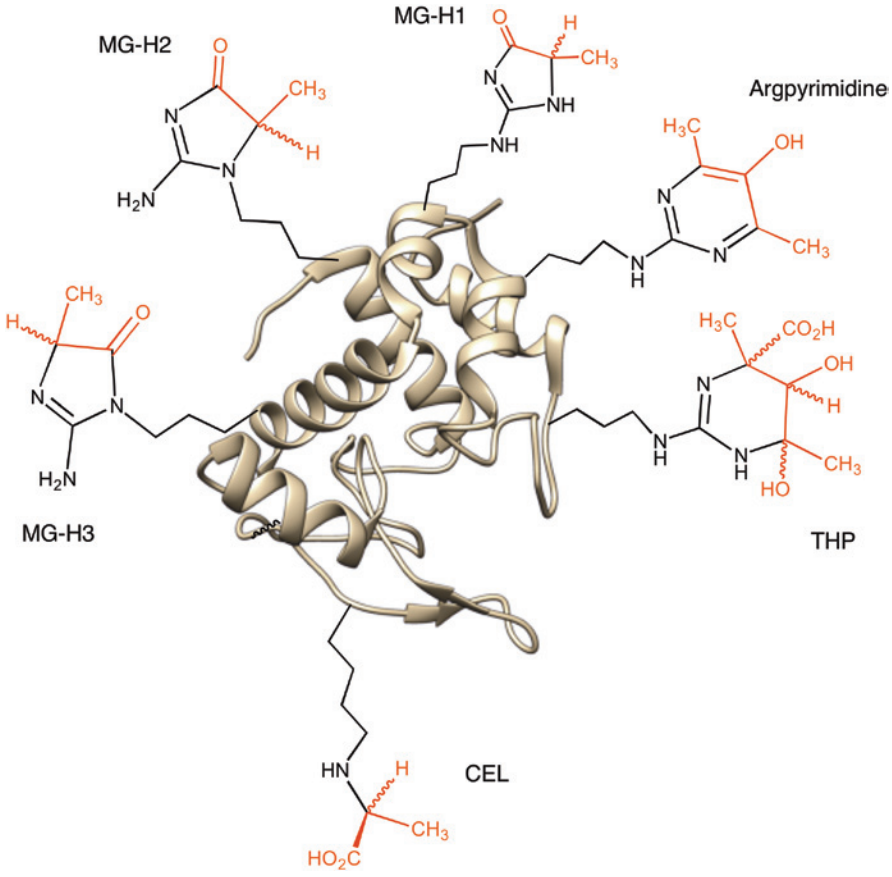

Figure 10: Chemical structures of identified MG-arginine and MG-lysine side chain protein adducts formed from advanced glycation end-product (AGE) formation. Atoms colored in red originate from MG.

argpyrimidine (1). A less frequently found modification, that of lysine modification, results in the formation of N^{ε}-(carboxyethyl)lysine (CEL). Protein crosslinks have also been identified and include MG-lysine dimer (MOLD) and MG-derived imidazolium crosslinking (MODIC) crosslinks (14, 115) (Figure 11). DNA modification by MG can also occur and include adduct formation with deoxyguanosine nucleotides (110, 116, 117).

An intensely active area of current glyoxalase research is that of the correlation of MG, AGE and disease. Connections to vascular diseases, diabetic complications and diabetic neuropathy, and amyloid-type neurodegenerative disease, among other areas, are being investigated (13, 15, 118). In the area of vascular disease and diabetes, a recent study has reported that increased MG derived AGE appear to be associated with an increased risk of cardiovascular events in type 2 diabetic patients (119). Post-translationally glycated proteins are thought to exert their effects on cells by a receptor-mediated pathway that includes their interaction with a receptor recognizing AGE-modified proteins. The receptor, termed RAGE, is a member of the immunoglobulin superfamily of cell-surface receptors and specifically recognizes MG-modified AGEs (120). This interaction appears to result in cellular activation leading ultimately to inflammation-provoking tissue injury (13). AGEs produced by MG are believed to be an important molecular cause for pain associated with diabetic neuropathy due to the post-translational modification of ion channels in neurons that are contributors to chemosensation and action potential generation in nerve endings (121). A recent overview of the literature linking the potential health effects to the presence of MG and AGE indicates the wide-ranging physiological effects of these molecules (14).

It cannot be stated too strongly that the biochemical links between MG, biomolecule modification and resulting disease states are underpinned by excellent quality analytical identification and quantitation protocols (110, 122–128). The labile nature of DHAP and GAP can result in incorrect quantitation of MG levels in cells and tissues, the reactivity of MG and the non-permanence of AGE modifications add further complexities to this research

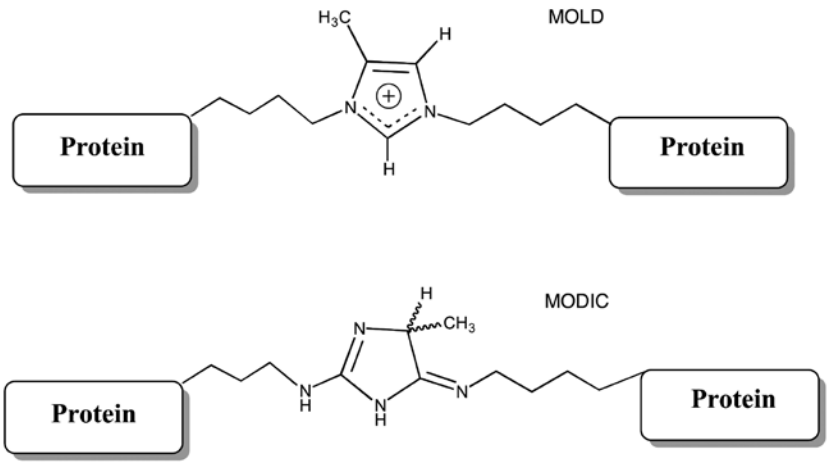

Figure 11: Chemical structures of identified protein crosslinks formed due to advanced glycation end-product reactions with MG.

area. Although challenging, investigations in these areas should prove intellectually as well as pragmatically rewarding well into the future.

Expert opinion

Substantial biochemical information has been obtained already on the enzymes involved in glyoxalase and MG biochemistry. Yet additional biochemical and structural investigations on new glyoxalase enzymes (Glo1, Glo2, Glo3) will allow for expanded understanding of metalloenzymes and the critical active site structures required to control metal activation profile and catalytic activity.

The identification of additional roles for MG and other dicarbonyls in biological tissues should be a future goal. The application of the current cadre of rigorous analytical methodology to identify and quantify dicarbonyl biomolecule modifications such as glycation and crosslinked biomolecules, termed AGE, should lead to a deeper understanding of the impact that these modifications have on tissues and organisms.

Outlook

It is likely that collaborative research on the enzymes that control the cellular concentration of dicarbonyls, and the further development of analytical techniques that better identify and quantitate the adducts formed by reaction of proteins and DNA with dicarbonyls will bring vastly improved appreciation for the underlying control and correction of certain diseases. This area will continue to focus on the chemistry and biochemistry of dicarbonyls and the additional fundamental knowledge will provide contributions to the understanding of a range of diseases, including cardiovascular disease and pain perception. Further advances in understanding the role of MG and the glyoxalase system in plants should be pivotal in improving crop yields and hence food stability

Highlights

- MG formation and degradation in the cell is now well understood
- advanced knowledge of the structure and function of enzymes that degrade MG in the cell is available
- knowledge of the detailed chemical mechanisms of the Glo1, Glo2 and Glo3 detoxification enzymes is improved although future work is necessary
- better understanding of metalloenzymes and how protein scaffolds control metal activation characteristics is available
- robust analytical techniques as applied to metabolite analysis and MG protein and DNA modification are available
- improved appreciation of AGE modifications as underlying contributors to various diseases is occurring

List of abbreviations

AGE	advanced glycation end-products
CEL	N^{ε}-(carboxyethyl)lysine
DHAP	dihydroxyacetone phosphate
EXAFS	extended X-ray absorption fine structure

GAP	glyceraldehyde-3-phosphate
Glo1	glyoxalase I
Glo2	glyoxalase II
Glo3	glyoxalase III
GSH	glutathione
Hsp	heat shock protein
MG	methylglyoxal
MODIC	methylglyoxal-derived imidazolium crosslinking
MOLD	methylglyoxal-derived lysine dimer
NADPH	nicotinamide adenine dinucleotide (phosphate) reduced
NMR	nuclear magnetic resonance
ORF	open reading frame
RAGE	receptor for advanced glycation end-products
RpoS	RNA polymerase sigma factor
THP	tetrahydropyrimidine
TIM	triose phosphate isomerase
XANES	X-ray absorption near edge structure.

Acknowledgments: The Natural Sciences and Engineering Research Council of Canada (NSERC), the Ontario Government and the University of Waterloo are gratefully acknowledged for financial support. The author has no financial or other conflict of interest in the writing of this article.

References

1. Sousa Silva M, Gomes RA, Ferreira AE, Ponces Freire A, Cordeiro C. The glyoxalase pathway: the first hundred years... and beyond. Biochem J 2013; 453: 1–15.
2. Thornalley PJ. The glyoxalase system: new developments towards functional characterization of a metabolic pathway fundamental to biological life. Biochem J 1990; 269: 1–11.
3. Racker E. The mechanism of action of glyoxalase. J Biol Chem 1951; 190: 685–96.
4. Crook EM, Law K. Glyoxalase; the role of the components. Biochem J 1952; 52: 492–9.
5. Thornalley PJ. Glyoxalase I-structure, function and a critical role in the enzymatic defence against glycation. Biochem Soc Trans 2003; 31: 1343–8.
6. Mannervik B, Ridderstrom M. Catalytic and molecular properties of glyoxalase I. Biochem Soc Trans 1993; 21: 515–7.
7. Aronsson AC, Marmstal E, Mannervik B. Glyoxalase I, a zinc metalloenzyme of mammals and yeast. Biochem Biophys Res Commun 1978; 81: 1235–40.
8. Suttisansanee U, Honek JF. Bacterial glyoxalase enzymes. Semin Cell Dev Biol 2011; 22: 285–92.
9. Sukdeo N, Honek JF. Microbial glyoxalase enzymes: metalloenzymes controlling cellular levels of methylglyoxal. Drug Metabol Drug Interact 2008; 23: 29–50.
10. Zhao Q, Su Y, Wang Z, Chen C, Wu T, Huang Y. Identification of glutathione (GSH)-independent glyoxalase III from *Schizosaccharomyces pombe*. BMC Evol Biol 2014; 14: 86.
11. Misra K, Banerjee AB, Ray S, Ray M. Glyoxalase III from *Escherichia coli*: a single novel enzyme for the conversion of methylglyoxal into D-lactate without reduced glutathione. Biochem J 1995; 305 (Pt 3): 999–1003.
12. Choi D, Kim J, Ha S, Kwon K, Kim EH, Lee HY, Ryu K.-S., Park C. Stereospecific mechanism of DJ-1 glyoxalases inferred from their hemithioacetal-containing crystal structures. FEBS J 2014; 281: 5447–62.
13. Schalkwijk CG. Vascular AGE-ing by methylglyoxal: the past, the present and the future. Diabetologia 2015; 58: 1715–9.
14. Rabbani N, Thornalley PJ. Dicarbonyl stress in cell and tissue dysfunction contributing to ageing and disease. Biochem Biophys Res Commun 2015; 458: 221–6.
15. Maessen DE, Stehouwer CD, Schalkwijk CG. The role of methylglyoxal and the glyoxalase system in diabetes and other age-related diseases. Clin Sci (Lond) 2015; 128: 839–61.
16. Rabbani N, Thornalley PJ. Dicarbonyl proteome and genome damage in metabolic and vascular disease. Biochem Soc Trans 2014; 42: 425–32.
17. Ahmed U, Thornalley PJ, Rabbani N. Possible role of methylglyoxal and glyoxalase in arthritis. Biochem Soc Trans 2014; 42: 538–42.
18. Beisswenger PJ. Methylglyoxal in diabetes: link to treatment, glycaemic control and biomarkers of complications. Biochem Soc Trans 2014; 42: 450–6.
19. Rabbani N, Thornalley PJ. Glyoxalase Centennial conference: introduction, history of research on the glyoxalase system and future prospects. Biochem Soc Trans 2014; 42: 413–8.
20. Rabbani N, Thornalley PJ. Methylglyoxal, glyoxalase 1 and the dicarbonyl proteome. Amino Acids 2012; 42: 1133–42.
21. Chakraborty S, Karmakar K, Chakravortty D. Cells producing their own nemesis: understanding methylglyoxal metabolism. IUBMB Life 2014; 66: 667–78.
22. Wyllie S, Fairlamb AH. Methylglyoxal metabolism in trypanosomes and leishmania. Semin Cell Dev Biol 2011; 22: 271–7.
23. Rabbani N, Thornalley PJ. The glyoxalase system–from microbial metabolism, through ageing to human disease and multidrug resistance. Semin Cell Dev Biol 2011; 22: 261.
24. Richard JP. Kinetic parameters for the elimination reaction catalyzed by triosephosphate isomerase and an estimation of the reaction's physiological significance. Biochemistry 1991; 30: 4581–5.
25. Phillips SA, Thornalley PJ. The formation of methylglyoxal from triose phosphates. Investigation using a specific assay for methylglyoxal. Eur J Biochem 1993; 212: 101–5.
26. Richard JP. Mechanism for the formation of methylglyoxal from triosephosphates. Biochem Soc Trans 1993; 21: 549–53.
27. Radjei S, Friguet B, Nizard C, Petropoulos I. Prevention of dicarbonyl-mediated advanced glycation by glyoxalases: implication in skin aging. Biochem Soc Trans 2014; 42: 518–22.
28. Suh KS, Choi EM, Rhee SY, Kim YS. Methylglyoxal induces oxidative stress and mitochondrial dysfunction in osteoblastic MC3T3-E1 cells. Free Radic Res 2014; 48: 206–17.
29. Ferguson GP, Totemeyer S, MacLean MJ, Booth IR. Methylglyoxal production in bacteria: suicide or survival? Arch Microbiol 1998; 170: 209–18.
30. Inoue Y, Kimura A. Methylglyoxal and regulation of its metabolism in microorganisms. Adv Microb Physiol 1995; 37: 177–227.
31. Cooper RA, Anderson A. The formation and catabolism of methylglyoxal during glycolysis in *Escherichia coli*. FEBS Lett 1970; 11: 273–6.
32. Lyles GA, Chalmers J. The metabolism of aminoacetone to methylglyoxal by semicarbazide-sensitive amine oxidase in human umbilical artery. Biochem Pharmacol 1992; 43: 1409–14.

33. Thornalley PJ. Pharmacology of methylglyoxal: formation, modification of proteins and nucleic acids, and enzymatic detoxification–a role in pathogenesis and antiproliferative chemotherapy. Gen Pharmacol 1996; 27: 565–73.
34. Koop DR, Casazza JP. Identification of ethanol-inducible P-450 isozyme 3a as the acetone and acetol monooxygenase of rabbit microsomes. J Biol Chem 1985; 260: 13607–12.
35. Aguilera J, Prieto JA. The *Saccharomyces cerevisiae* aldose reductase is implied in the metabolism of methylglyoxal in response to stress conditions. Curr Genet 2001; 39: 273–83.
36. Vander Jagt DL, Hassebrook RK, Hunsaker LA, Brown WM, Royer RE. Metabolism of the 2-oxoaldehyde methylglyoxal by aldose reductase and by glyoxalase-I: roles for glutathione in both enzymes and implications for diabetic complications. Chem Biol Interact 2001; 130–132: 549–62.
37. Vander Jagt DL, Hunsaker LA. Methylglyoxal metabolism and diabetic complications: roles of aldose reductase, glyoxalase-I, betaine aldehyde dehydrogenase and 2-oxoaldehyde dehydrogenase. Chem Biol Interact 2003; 143–144: 341–51.
38. Ko J, Kim I, Yoo S, Min B, Kim K, Park C. Conversion of methylglyoxal to acetol by *Escherichia coli* aldo-keto reductases. J Bacteriol 2005; 187: 5782–9.
39. Murata K, Fukuda Y, Simosaka M, Watanabe K, Saikusa T, Kimura A. Metabolism of 2-oxoaldehyde in yeasts. Purification and characterization of NADPH-dependent methylglyoxal-reducing enzyme from *Saccharomyces cerevisiae*. Eur J Biochem 1985; 151: 631–6.
40. Inoue Y, Rhee H, Watanabe K, Murata K, Kimura A. Metabolism of 2-oxoaldehyde in mold. Purification and characterization of two methylglyoxal reductases from *Aspergillus niger*. Eur J Biochem 1988; 171: 213–8.
41. Ray M, Ray S. Purification and partial characterization of a methylglyoxal reductase from goat liver. Biochim Biophys Acta 1984; 802: 119–27.
42. Liyanage H, Kashket S, Young M, Kashket ER. *Clostridium beijerinckii* and *Clostridium difficile* detoxify methylglyoxal by a novel mechanism involving glycerol dehydrogenase. Appl Environ Microb 2001; 67: 2004–10.
43. Greig N, Wyllie S, Patterson S, Fairlamb AH. A comparative study of methylglyoxal metabolism in trypanosomatids. FEBS J 2009; 276: 376–86.
44. Deponte M. Glyoxalase diversity in parasitic protists. Biochem Soc Trans 2014; 42: 473–8.
45. Mannervik B. Molecular enzymology of the glyoxalase system. Drug Metab Drug Interact 2008; 23: 13–27.
46. Honek JF. Bacterial glyoxalase I enzymes: structural and biochemical investigations. Biochem Soc Trans 2014; 42: 479–84.
47. Lages NF, Cordeiro C, Sousa Silva M, Ponces Freire A, Ferreira AE. Optimization of time-course experiments for kinetic model discrimination. PLoS One 2012; 7: e32749.
48. Vickers TJ, Greig N, Fairlamb AH. A trypanothione-dependent glyoxalase I with a prokaryotic ancestry in *Leishmania major*. Proc Natl Acad Sci USA 2004; 101: 13186–91.
49. Sousa Silva M, Ferreira AE, Gomes R, Tomas AM, Ponces Freire A, Cordeiro C. The glyoxalase pathway in protozoan parasites. Int J Med Microbiol 2012; 302: 225–9.
50. Kimura A, Inoue Y. Glyoxalase I in micro-organisms: molecular characteristics, genetics and biochemical regulation. Biochem Soc Trans 1993; 21: 518–22.
51. Ridderstrom M, Mannervik B. The primary structure of monomeric yeast glyoxalase I indicates a gene duplication resulting in two similar segments homologous with the subunit of dimeric human glyoxalase I. Biochem J 1996; 316 (Pt 3): 1005–6.
52. Saint-Jean AP, Phillips KR, Creighton DJ, Stone MJ. Active monomeric and dimeric forms of *Pseudomonas putida* glyoxalase I: evidence for 3D domain swapping. Biochemistry 1998; 37: 10345–53.
53. Sellin S, Mannervik B. Metal dissociation constants for glyoxalase I reconstituted with Zn^{2+}, Co^{2+}, Mn^{2+}, and Mg^{2+}. J Biol Chem 1984; 259: 11426–9.
54. Cameron AD, Olin B, Ridderstrom M, Mannervik B, Jones TA. Crystal structure of human glyoxalase I–evidence for gene duplication and 3D domain swapping. EMBO J 1997; 16: 3386–95.
55. Rosevear PR, Chari RV, Kozarich JW, Sellin S, Mannervik B, Mildvan AS. 13C NMR studies of the product complex of glyoxalase I. J Biol Chem 1983; 258: 6823–6.
56. Sellin S, Eriksson LE, Aronsson AC, Mannervik B. Octahedral metal coordination in the active site of glyoxalase I as evidenced by the properties of Co(II)-glyoxalase I. J Biol Chem 1983; 258: 2091–3.
57. Rosevear PR, Sellin S, Mannervik B, Kuntz ID, Mildvan AS. NMR and computer modeling studies of the conformations of glutathione derivatives at the active site of glyoxalase I. J Biol Chem 1984; 259: 11436–47.
58. Clugston SL, Barnard JF, Kinach R, Miedema D, Ruman R, Daub E, Honek, JF. Overproduction and characterization of a dimeric non-zinc glyoxalase I from *Escherichia coli*: evidence for optimal activation by nickel ions. Biochemistry 1998; 37: 8754–63.
59. Davidson G, Clugston SL, Honek JF, Maroney MJ. XAS investigation of the nickel active site structure in *Escherichia coli* glyoxalase I. Inorg Chem 2000; 39: 2962–3.
60. Davidson G, Clugston SL, Honek JF, Maroney MJ. An XAS investigation of product and inhibitor complexes of Ni-containing GlxI from *Escherichia coli*: mechanistic implications. Biochemistry 2001; 40: 4569–82.
61. He MM, Clugston SL, Honek JF, Matthews BW. Determination of the structure of *Escherichia coli* glyoxalase I suggests a structural basis for differential metal activation. Biochemistry 2000; 39: 8719–27.
62. Su Z, Sukdeo N, Honek JF. 15N-1H HSQC NMR evidence for distinct specificity of two active sites in *Escherichia coli* glyoxalase I. Biochemistry 2008; 47: 13232–41.
63. Clugston SL, Yajima R, Honek JF. Investigation of metal binding and activation of *Escherichia coli* glyoxalase I: kinetic, thermodynamic and mutagenesis studies. Biochem J 2004; 377: 309–16.
64. Mullings KY, Sukdeo N, Suttisansanee U, Ran Y, Honek JF. Ni2+-activated glyoxalase I from *Escherichia coli*: substrate specificity, kinetic isotope effects and evolution within the $\beta\alpha\beta\beta\beta$ superfamily. J Inorg Biochem 2012; 108: 133–40.
65. Greig N, Wyllie S, Vickers TJ, Fairlamb AH. Trypanothione-dependent glyoxalase I in *Trypanosoma cruzi*. Biochem J 2006; 400: 217–23.
66. Padmanabhan PK, Mukherjee A, Singh S, Chattopadhyaya S, Gowri VS, Myler PJ, Srinivasan N, Madhubala R. Glyoxalase I from *Leishmania donovani*: a potential target for anti-parasite drug. Biochem Biophys Res Commun 2005; 337: 1237–48.
67. Chandrangsu P, Dusi R, Hamilton CJ, Helmann JD. Methylglyoxal resistance in *Bacillus subtilis*: contributions of bacillithiol-

dependent and independent pathways. Mol Microbiol 2014; 91: 706–15.
68. Sukdeo N, Clugston SL, Daub E, Honek JF. Distinct classes of glyoxalase I: metal specificity of the *Yersinia pestis*, *Pseudomonas aeruginosa* and *Neisseria meningitidis* enzymes. Biochem J 2004; 384: 111–7.
69. Sukdeo N, Honek JF. *Pseudomonas aeruginosa* contains multiple glyoxalase I-encoding genes from both metal activation classes. Biochim Biophys Acta 2007; 1774: 756–63.
70. Bythell-Douglas R, Suttisansanee U, Flematti GR, Challenor M, Lee M, Panjikar S, Honek JF, Bond CS. The crystal structure of a homodimeric *Pseudomonas* glyoxalase I enzyme reveals asymmetric metallation commensurate with half-of-sites activity. Chemistry 2015; 21: 541–4.
71. Suttisansanee U, Ran Y, Mullings KY, Sukdeo N, Honek JF. Modulating glyoxalase I metal selectivity by deletional mutagenesis: underlying structural factors contributing to nickel activation profiles. Metallomics 2015; 7: 605–12.
72. Suttisansanee U, Lau K, Lagishetty S, Rao KN, Swaminathan S, Sauder JM, Burley SK, Honek JF. Structural variation in bacterial glyoxalase I enzymes: investigation of the metalloenzyme glyoxalase I from *Clostridium acetobutylicum*. J Biol Chem 2011; 286: 38367–74.
73. Marmstal E, Aronsson AC, Mannervik B. Comparison of glyoxalase I purified from yeast (*Saccharomyces cerevisiae*) with the enzyme from mammalian sources. Biochem J 1979; 183: 23–30.
74. Iozef R, Rahlfs S, Chang T, Schirmer H, Becker K. Glyoxalase I of the malarial parasite *Plasmodium falciparum*: evidence for subunit fusion. FEBS Lett 2003; 554: 284–8.
75. Deponte M, Sturm N, Mittler S, Harner M, Mack H, Becker K. Allosteric coupling of two different functional active sites in monomeric *Plasmodium falciparum* glyoxalase I. J Biol Chem 2007; 282: 28419–30.
76. Mustafiz A, Ghosh A, Tripathi AK, Kaur C, Ganguly AK, Bhavesh NS, Tripathi JK, Pareek A, Sopory SK, Singla-Pareek SL. A unique Ni2+ -dependent and methylglyoxal-inducible rice glyoxalase I possesses a single active site and functions in abiotic stress response. Plant J 2014; 78: 951–63.
77. Shimakawa G, Suzuki M, Yamamoto E, Saito R, Iwamoto T, Nishi A, Miyake C. Why don't plants have diabetes? Systems for scavenging reactive carbonyls in photosynthetic organisms. Biochem Soc Trans 2014; 42: 543–7.
78. Kaur C, Ghosh A, Pareek A, Sopory SK, Singla-Pareek SL. Glyoxalases and stress tolerance in plants. Biochem Soc Trans 2014; 42: 485–90.
79. Kaur C, Vishnoi A, Ariyadasa TU, Bhattacharya A, Singla-Pareek SL, Sopory SK. Episodes of horizontal gene-transfer and gene-fusion led to co-existence of different metal-ion specific glyoxalase I. Sci Rep 2013; 3: 3076.
80. Armstrong RN. Mechanistic diversity in a metalloenzyme superfamily. Biochemistry 2000; 39: 13625–32.
81. Bergdoll M, Eltis LD, Cameron AD, Dumas P, Bolin JT. All in the family: structural and evolutionary relationships among three modular proteins with diverse functions and variable assembly. Protein Sci 1998; 7: 1661–70.
82. Bernat BA, Laughlin LT, Armstrong RN. Fosfomycin resistance protein (FosA) is a manganese metalloglutathione transferase related to glyoxalase I and the extradiol dioxygenases. Biochemistry 1997; 36: 3050–5.
83. Dumas P, Bergdoll M, Cagnon C, Masson JM. Crystal structure and site-directed mutagenesis of a bleomycin resistance protein and their significance for drug sequestering. EMBO J 1994; 13: 2483–92.
84. Martin TW, Dauter Z, Devedjiev Y, Sheffield P, Jelen F, He M, Sherman DH, Otlewski J, Derewenda ZS, Derewenda U. Molecular basis of mitomycin C resistance in *streptomyces*: structure and function of the MRD protein. Structure 2002; 10: 933–42.
85. Biswas T, Zolova OE, Lombo F, de la Calle F, Salas JA, Tsodikov OV, Garneau-Tsodikova S. A new scaffold of an old protein fold ensures binding to the bisintercalator thiocoraline. J Mol Biol 2010; 397: 495–507.
86. Thompson MK, Keithly ME, Harp J, Cook PD, Jagessar KL, Sulikowski GA, Armstrong RN. Structural and chemical aspects of resistance to the antibiotic fosfomycin conferred by FosB from *Bacillus cereus*. Biochemistry 2013; 52: 7350–62.
87. Fillgrove KL, Pakhomova S, Schaab MR, Newcomer ME, Armstrong RN. Structure and mechanism of the genomically encoded fosfomycin resistance protein, FosX, from *Listeria monocytogenes*. Biochemistry 2007; 46: 8110–20.
88. Cameron AD, Ridderstrom M, Olin B, Mannervik B. Crystal structure of human glyoxalase II and its complex with a glutathione thiolester substrate analogue. Structure 1999; 7: 1067–78.
89. Marasinghe GP, Sander IM, Bennett B, Periyannan G, Yang KW, Makaroff CA, Crowder MW. Structural studies on a mitochondrial glyoxalase II. J Biol Chem 2005; 280: 40668–75.
90. Trincao J, Sousa Silva M, Barata L, Bonifacio C, Carvalho S, Tomas AM, Ferreira AEN, Cordeiro C, Freire AP, Romão MJ. Purification, crystallization and preliminary X-ray diffraction analysis of the glyoxalase II from *Leishmania infantum*. Acta Crystallogr Sect F Struct Biol Cryst Commun 2006; 62: 805–7.
91. Campos-Bermudez VA, Leite NR, Krog R, Costa-Filho AJ, Soncini FC, Oliva G, Vila AJ. Biochemical and structural characterization of *Salmonella typhimurium* glyoxalase II: new insights into metal ion selectivity. Biochemistry 2007; 46: 11069–79.
92. Talesa V, Rosi G, Contenti S, Mangiabene C, Lupattelli M, Norton SJ, Giovannini E, Principato GB. Presence of glyoxalase II in mitochondria from spinach leaves: comparison with the enzyme from cytosol. Biochem Int 1990; 22: 1115–20.
93. Bito A, Haider M, Briza P, Strasser P, Breitenbach M. Heterologous expression, purification, and kinetic comparison of the cytoplasmic and mitochondrial glyoxalase II enzymes, Glo2p and Glo4p, from *Saccharomyces cerevisiae*. Protein Expr Purif 1999; 17: 456–64.
94. Wenzel NF, Carenbauer AL, Pfiester MP, Schilling O, Meyer-Klaucke W, Makaroff CA, Crowder MW. The binding of iron and zinc to glyoxalase II occurs exclusively as di-metal centers and is unique within the metallo-beta-lactamase family. J Biol Inorg Chem 2004; 9: 429–38.
95. Schilling O, Wenzel N, Naylor M, Vogel A, Crowder M, Makaroff C, Meyer-Klaucke W. Flexible metal binding of the metallo-b-lactamase domain: glyoxalase II incorporates iron, manganese, and zinc *in vivo*. Biochemistry 2003; 42: 11777–86.
96. Limphong P, McKinney RM, Adams NE, Bennett B, Makaroff CA, Gunasekera T, Crowder MW. Human glyoxalase II contains an Fe(II)Zn(II) center but is active as a mononuclear Zn(II) enzyme. Biochemistry 2009; 48: 5426–34.
97. O'Young J, Sukdeo N, Honek JF. *Escherichia coli* glyoxalase II is a binuclear zinc-dependent metalloenzyme. Arch Biochem Biophys 2007; 459: 20–6.

98. Reiger M, Lassak J, Jung K. Deciphering the role of the type II glyoxalase isoenzyme YcbL (GlxII-2) in *Escherichia coli*. FEMS Microbiol Lett 2015; 362: 1–7.
99. Crowder MW, Maiti MK, Banovic L, Makaroff CA. Glyoxalase II from *A. thaliana* requires Zn(II) for catalytic activity. FEBS Lett 1997; 418: 351–4.
100. Daiyasu H, Osaka K, Ishino Y, Toh H. Expansion of the zinc metallo-hydrolase family of the b-lactamase fold. FEBS Lett 2001; 503: 1–6.
101. Baier F, Chen J, Solomonson M, Strynadka NC, Tokuriki N. Distinct metal isoforms underlie promiscuous activity profiles of metalloenzymes. ACS Chem Biol 2015; 10: 1684–93.
102. Park HS, Nam SH, Lee JK, Yoon CN, Mannervik B, Benkovic SJ, Kim HS. Design and evolution of new catalytic activity with an existing protein scaffold. Science 2006; 311: 535–8.
103. Benov L, Sequeira F, Beema AF. Role of rpoS in the regulation of glyoxalase III in *Escherichia coli*. Acta Biochim Pol 2004; 51: 857–60.
104. Subedi KP, Choi D, Kim I, Min B, Park C. Hsp31 of *Escherichia coli* K-12 is glyoxalase III. Mol Microbiol 2011; 81: 926–36.
105. Lee JY, Song J, Kwon K, Jang S, Kim C, Baek K, Kim J, Park C. Human DJ-1 and its homologs are novel glyoxalases. Hum Mol Genet 2012; 21: 3215–25.
106. Quigley PM, Korotkov K, Baneyx F, Hol WG. The 1.6-A crystal structure of the class of chaperones represented by *Escherichia coli* Hsp31 reveals a putative catalytic triad. Proc Natl Acad Sci USA 2003; 100: 3137–42.
107. Kalapos MP. Special issue on methylglyoxal. Preface. Drug Metab Drug Interact 2008; 23: 1.
108. Ramasamy R, Yan SF, Schmidt AM. Advanced glycation end-products: from precursors to RAGE: round and round we go. Amino Acids 2012; 42: 1151–61.
109. Biemel KM, Friedl DA, Lederer MO. Identification and quantification of major maillard cross-links in human serum albumin and lens protein. Evidence for glucosepane as the dominant compound. J Biol Chem 2002; 277: 24907–15.
110. Rabbani N, Shaheen F, Anwar A, Masania J, Thornalley PJ. Assay of methylglyoxal-derived protein and nucleotide AGEs. Biochem Soc Trans 2014; 42: 511–7.
111. Hanssen NM, Wouters K, Huijberts MS, Gijbels MJ, Sluimer JC, Scheijen JL, Heeneman S, Biessen EA, Daemen MJ, Brownlee M, de Kleijn DP, Stehouwer CD, Pasterkamp G, Schalkwijk CG. Higher levels of advanced glycation endproducts in human carotid atherosclerotic plaques are associated with a rupture-prone phenotype. Eur Heart J 2014; 35: 1137–46.
112. Rabbani N, Thornalley PJ. The dicarbonyl proteome: proteins susceptible to dicarbonyl glycation at functional sites in health, aging, and disease. Ann N Y Acad Sci 2008; 1126: 124–7.
113. Oya T, Hattori N, Mizuno Y, Miyata S, Maeda S, Osawa T, Uchida K. Methylglyoxal modification of protein. Chemical and immunochemical characterization of methylglyoxal-arginine adducts. J Biol Chem 1999; 274: 18492–502.
114. Papoulis A, al-Abed Y, Bucala R. Identification of N2-(1-carboxyethyl)guanine (CEG) as a guanine advanced glycosylation end product. Biochemistry 1995; 34: 648–55.
115. Biemel KM, Conrad J, Lederer MO. Unexpected carbonyl mobility in aminoketoses: the key to major Maillard crosslinks. Angew Chem Int Ed Engl 2002; 41: 801–4.
116. Thornalley PJ. Protecting the genome: defence against nucleotide glycation and emerging role of glyoxalase I overexpression in multidrug resistance in cancer chemotherapy. Biochem Soc Trans 2003; 31: 1372–7.
117. Thornalley PJ. Endogenous a-oxoaldehydes and formation of protein and nucleotide advanced glycation endproducts in tissue damage. Novartis Found Symp 2007; 285: 229–43; discussion 43–6.
118. Krautwald M, Munch G. Advanced glycation end products as biomarkers and gerontotoxins - a basis to explore methylglyoxal-lowering agents for Alzheimer‘s disease? Exp Gerontol 2010; 45: 744–51.
119. Hanssen NM, Beulens JW, van Dieren S, Scheijen JL, van der AD, Spijkerman AM, van der Schouw YT, Stehouwer CD, Schalkwijk CG. Plasma advanced glycation end products are associated with incident cardiovascular events in individuals with type 2 diabetes: a case-cohort study with a median follow-up of 10 years (EPIC-NL). Diabetes 2015; 64: 257–65.
120. Xue J, Ray R, Singer D, Bohme D, Burz DS, Rai V, Hoffmann R, Shekhtman A. The receptor for advanced glycation end products (RAGE) specifically recognizes methylglyoxal-derived AGEs. Biochemistry 2014; 53: 3327–35.
121. Fleming T, Nawroth PP. Reactive metabolites as a cause of late diabetic complications. Biochem Soc Trans 2014; 42: 439–42.
122. McLellan AC, Phillips SA, Thornalley PJ. The assay of methylglyoxal in biological systems by derivatization with 1,2-diamino-4,5-dimethoxybenzene. Anal Biochem 1992; 206: 17–23.
123. McLellan AC, Phillips SA, Thornalley PJ. Fluorimetric assay of D-lactate. Anal Biochem 1992; 206: 12–6.
124. Xue M, Rabbani N, Thornalley PJ. Measurement of glyoxalase gene expression. Biochem Soc Trans 2014; 42: 495–9.
125. Thornalley PJ, Rabbani N. Assay of methylglyoxal and glyoxal and control of peroxidase interference. Biochem Soc Trans 2014; 42: 504–10.
126. Shaheen F, Shmygol A, Rabbani N, Thornalley PJ. A fluorogenic assay for methylglyoxal. Biochem Soc Trans 2014; 42: 548–55.
127. Rabbani N, Thornalley PJ. Measurement of methylglyoxal by stable isotopic dilution analysis LC-MS/MS with corroborative prediction in physiological samples. Nat Protoc 2014; 9: 1969–79.
128. Arai M, Nihonmatsu-Kikuchi N, Itokawa M, Rabbani N, Thornalley PJ. Measurement of glyoxalase activities. Biochem Soc Trans 2014; 42: 491–4.